Garmultin-A Incites Apoptosis in CB3 Cells Through miR-17-5p by Attenuating Poly (ADP-Ribose) Polymerase-1

Jianfei Qiu[1,2,3], **Li Chen**[1,2], **Jue Yang**[1,2], **Krishnapriya M. Varier**[1,2], **Babu Gajendran**[1,2], **Yao Yao**[1,2], **Wuling Liu**[1,2], **Jingrui Song**[1,2], **Qing Rao**[1,2], **Qun Long**[1,2], **Chunmao Yuan**[1,2], **Xiaojiang Hao**[1,2], and **Yanmei Li**[1,2]

Abstract

Background: Leukemia accounts for a large number of deaths, worldwide, every year. Treating this ailment is always a challenging job. Recently, oncogenic miRNA leading to apoptosis are highly promising targets of many natural products. In this study, Garmultin-A (GA), isolated from the bark of *Garcinia multiflora*, was elucidated for its anti-leukemic effect in CB3 cells.

Methods: The effect of the compound on CB3 cell viability was detected by MTT assay and apoptosis by FITC Annexin V/PI and Hochest 33258 staining. The western blot analysis assessed the BAX, BCL2, cMYC, pERK, and PARP-1 protein levels. Autodock analysis predicted the ligand–protein interactions. q-RT-PCR quantified the miR-17-5p expression. Luciferase assay confirmed the interaction between PARP-1 and miR-17-5p.

Results: We uncover that GA leads to apoptosis by inducing overexpression of miR-17-5p and significantly downregulate PARP-1 protein levels in CB3 cells. The overexpression of miR-17-5p promotes apoptosis, and the miR-17-5p antagomirs restore GA-triggered apoptosis. Notably, we disclose that PARP-1 is a direct target of miR-17-5p. Increased pro-apoptotic and reduced anti-apoptosis protein levels were also observed in GA-treated CB3 cells.

Conclusion: These results provide critical insights that GA could induce apoptosis in CB3 cells through targeting miR-17-5p by attenuating PARP-1. Thus, GA could act as a novel therapeutic agent for erythroleukemia.

Keywords

Garmultin-A, leukemia, apoptosis, miR-17-5p, PARP-1

Introduction

Leukemia is one of the foremost causes of death due to blood malignancies in the human population worldwide.[1] Natural products obtained from medicinal plants can provide changes like DNA methylation and histone arrangements, causing alterations in cellular signaling, epigenetically.[2] These epigenetic changes may lead to either inhibition of the activity of

[1] State Key Laboratory for Functions and Applications of Medicinal Plants/School of Pharmaceutical Sciences, Guizhou Medical University, Guiyang, P.R. China
[2] The Key Laboratory of Chemistry for Natural Products of Guizhou Province and Chinese Academic of Sciences, Guiyang, P.R. China
[3] Department of Immunology, College of Basic Medical Sciences, Guizhou Medical University, Guiyang, P.R. China

Corresponding Authors:
Chunmao Yuan, Xiaojiang Hao and Yanmei Li, State Key Laboratory for Functions and Applications of Medicinal Plants/School of Pharmaceutical Sciences, Guizhou Medical University, Baiyun District, Guiyang Guiyang, P.R. China.
Emails: yuanchunmao01@126.com; haoxj@mail.kib.ac.cn; liyanmei518@hotmail.com

onco-miRNAs or an increase in the expression of tumor suppressor miRNAs, which may finally inhibit cell proliferation through the induction of apoptosis.[3,4] Recently, plant bioactive compounds are of high-throughput screening for the prevention and treatment of many cancers.[5,6] Several scientific pieces of evidence have shown that many natural compounds exert anticancer effects via affecting the expression of many miRNAs, indicating that the regulation of miRNAs by natural products could be a novel strategy in cancer therapy.[6] In this context, it is relevant to mention that the genus Garcinia (Guttiferae) is a genus reported to have several polycyclic polyprenylated acylphloroglucinols (PPAPs), xanthones, and flavonoids with a broad array of biological activities. In particular, for the lung cancer Phase II clinical trials, gambogic acid from *Garcinia hanburyi* was approved. Moreover, the bark of *Garcinia multiflora* is applied externally to reduce inflammation.[7] Our previous study had obtained a series of novel PPAPs with good cytotoxic activity. Garmultin-A (GA) is one among those poly adenosine diphosphate-ribose polymerases (PARPs) with good cytotoxic activity against many cancer cells.[8]

The miRNAs are non-protein-coding small RNAs, a group of highly conserved 18–25 nucleotides, that repress mRNA translation or trigger mRNA degradation through binding to 3ʹ Un-Translated Regions (3ʹUTR) of target mRNAs.[9] It estimated that miRNAs regulate over 60% of all human genes.[10] The miRNAs directly regulate different biological processes that include proliferation and differentiation via affecting the expression of target genes.[11] MiR-17-5p is a member of miR-17-92 cluster, which is a polycistronic miRNA gene encoding seven individual miRNAs, namely, miR-17-5p, miR-17-3p, miR-18a, miR-19a, miR-20a, miR-19b, and miR-92a.[12,13] Plenty of evidence demonstrates the overexpression of miR-17~92 clusters in hematologic malignancies and lung cancers. Its enhanced expression experimentally triggers tumor growth by targeting tumor suppressors.[14] However, several other studies suggested that the deletion of miR-17~92 cluster was observed in ovarian cancer patients.[15] The miR-17-5p can act as both an onco-miRNA and a tumor suppressor in different cellular contexts. Specific overexpression of miR-17-5p blocks tumor cell growth and induces apoptosis by directly targeting oncogenes.[16] Moreover, CircTLK1-mediated sponging of miR-17-5p could result in cardiomyocyte apoptosis through mitochondrial damage by oxidative stress.[17] Thus, in this study, we have hypothesized to uncover the molecular target of GA that promotes cellular apoptosis in CB3 cells, which could be a novel anti-cancer agent for erythroleukemia.

Methods

Cell Line and Plant Materials

GA was isolated and characterized according to our previous work by Tian et al, 2016.[9] CB3 mouse erythroleukemia cell line

and HL-7702 non-tumor lineage cells were obtained from the University of Toronto.[18] The cells were well-bred in RPMI with 5% fetal bovine serum, 2 mmol/l L-glutamine, 100 U/ml penicillin, and 100 g/mL streptomycin (RPMI). Cells were incubated at 37°C in 5% CO_2 with 95% air humidified atmosphere. All the chemicals used in the study are of analytical grade.

Cell Cytotoxicity Assay

MTT (3-(4,5-dimethyl-thiazol-2yl)-2,5-diphenyl tetrazolium bromide) colorimetric assay was employed to determine cell viability.[19] Logarithmic growth cells were harvested, resuspended in fresh medium containing 10% fetal bovine serum, and inoculated into 96 wells at a rate of about 8×10^3 cells per well. After 24 h, cells were treated with GA at the concentrations of 1.25, 2.5, 5, 10, and 20 μM, with DMSO control. After 48 h of drug addition, 10 μL of MTT (5 mg/mL; Beyotime Biotechnology, Beijing, China) was added, and the treated cells were cultured for another four hours. Later, the supernatant was removed by centrifugation, followed by the addition of 160 μL of DMSO to each well, and shaken horizontally until the precipitate completely dissolved. Later, the microplate was read at 490 nm in a microplate reader (Biotek USA).

Cell-Growth Curves

Once the CB3 cells reached around 80% of confluence, they were counted in a cell counting chamber at 1:2 dilution with trypan blue dye exclusion (purchased from SIGMA-Aldrich). Around 5×10^3 CB3 cells per well were cultured in a 96-well plate to determine the proliferation parameters by the MTT method as described by Mosmann.[17] The growth curves developed as per Ramírez.[18] The cellular morphology changes on the treated cells were photographed in Nikon inverted microscope, according to Gajendran et al, 2020.[19]

Flow Cytometry Analysis

The apoptotic effects of GA against CB3 cells were examined by a FITC Annexin V and PI apoptosis detection kit I (BD Pharmingen™, USA) according to the manufacturer's protocol. In brief, cells were treated (5×10^4/well) with 2.5, 5, and 10 μM of the compound for 24 and 48 h, harvested by centrifuging at 3000 r/min for 15 min. Later, the pellets were collected and washed in 100 μL of binding buffer. The specific binding of FITC Annexin V was achieved by incubating cells in 100 μL of binding buffer at room temperature for 15 min in the dark and then immediately analyzed by NovoCyte flow cytometry (ACEA NovoCyte, USA) and interpreted using NovoExpress software. Untreated cells served as a negative control.[20]

Hochest 33258 Staining

The evaluation of the apoptotic cells was performed using Hochest 33258 staining.[21] The CB3 cells at its logarithmic

phase at the density of 2×10^4 cells/well were seeded explicitly in 24-well plates. After CB3 cells were treated with 0, 2.5, 5, and 10 μM of GA at 24 and 48 h of incubation, cells in the plates were centrifuged for 30 min at room temperature, followed by washing and staining with Hoechst 33258 at 37°C for 30 min. Later, the apoptotic cells were viewed by Nikon fluorescence microscope equipped with a UV filter and photographed.

Western Blot Analysis

CB3 cells treated with 5 and 10 μM of GA for 48 h were harvested and lysed.[22] Proteins separated by 10% SDS/PAGE and transferred to nitrocellulose membranes. Afterward, the membranes were blocked by 5% non-fat milk and then incubated with rabbit polyclonal anti-BCL2 (1: 2000; ab32124; Abcam, USA), anti-BAX (1: 2000; ab32503; Abcam, USA), anti-pERK (1: 2000; #4370T; Cell Signaling Technology, USA), anti cMYC (1: 2000; #13987; Cell Signaling Technology, USA), anti-PARP-1 (1: 2000; ab191217; Abcam, USA), and β-actin (#4967S, Cell Signaling Technology, USA). The immunoblots were rinsed three times with TBS/TBS-T buffer, incubated with the secondary antibody (Anti-rabbit IgG (H+L) (DyLight™ 800 4X PEG Conjugate; #5151P; Cell Signaling Technology), and analyzed by enhanced IR fluorescence with Li-Cor/Odyssey infrared image system (LI-COR Biosciences, Lincoln, NE, USA). β-actin served as an internal control for total protein levels. Relative fluorescence levels were determined by dividing the normalized fluorescence readings of the bands of interest by the corresponding β-actin loading control band of each sample.

Autodock Analysis

The molecular docking studies were conducted, according to Krishnapria et al, 2016.[23] The 3-D structures of venetoclax, MLS006011554, and ravoxertinib were retrieved from PubChem and optimized for docking using the Discovery Studio. The structure of the GA was drawn in Chem-sketch. The protein crystallographic structures of receptors BCL2, pERK, and cMYC were retrieved from www.rcsb.org and prepared for docking using Discovery Studio. Then the obtained structures were used for the docking studies (Autodock 4.2).

Quantitative Real-Time PCR

CB3 cells were cultured in the presence of GA or DMSO (control), and the total RNA was extracted with TRIzol® reagent (Invitrogen, Carlsbad, CA, USA). An equal amount of RNA (1 μg) was reverse transcribed to cDNA using the HiFi Script cDNA Synthesis Kit (Takara, Dalian, China). A quantitative real-time PCR (Ultra SYBR Mixture with High ROX) performed in a StepOnePlus TM Real-time PCR System (Thermo Fisher Scientific, Waltham, MA, USA). miR-specific primers were used for the analysis of the expression of mature miR-17-5p, keeping β-actin as internal control.[24]

Lentivirus Vector Construction

For cloning purposes, precursor overhang sequences from 5ɪ NotI- and 3ɪ XhoI-restriction sites having specific gene primers (Forward primer TCTATTTCAAATTTAGCAG-GAAAAA, Reverse primer GCACTCAACATCAGCAGG) were amplified to generate lentiviruses. The PCR products inserted into the lentiviral expression vector (pGFP-C-vector) generate pGFP-C-lenti-miR-17-5p. The confirmation of the insertions was performed using DNA sequencing of the plasmids. Anti-miR-17-5p was designed with the RNAi design algorithm for type 5 shRNA to generate miR-17-5p loss-of-function phenotypes. It was cloned into the BamHI and BsmBI sites of a modified pGFP-C-shLenti-miR (OriGene) to generate pGFP-C-shLenti-miR-17-5p.[24]

Virus Generation

The generation of lentiviruses was performed by co-transfecting lentiviral vector (5 mg), with packaging plasmids (6 mg), in 293T cells, by lipofectamine 2000 reagent having Lenti-shRNA of miR-17-5p. After 48 h of incubation, cells were centrifuged (3000 r/min/min), and supernatants were pooled. The collected supernatant was filtered (.45 μm) and used to infect cells.[24]

Lentiviral Transduction of CB3 Cells

Transfections were carried out as previously described.[24] In brief, CB3 cells (2×10^5) were immersed in 3 mL medium in each well of a 6-well plate after adding .5 mL of lentiviral particles with polyarginine (Sigma) for 20 min.[24]

Luciferase Assay

Luciferase assay was carried out as previously described.[24] In brief, NIH-3T3 cells (4×10^5) were seeded into 12-well plates. After 24 h, .2 mg of p MIR-REPORT Luciferase Reporter Plasmid expressing wild-type or mutated miR-17-5p binding sites in PARP1 3ɪ-untranslated regions (3ɪ-UTRs) and .8 mg pGFP-C-shlenti-miR-17-5p plasmid were added to each well using lipofectamine 2000 in triplicates. The Quick Change XL Mutagenesis Kit is used to perform mutagenesis of miR binding sites.[24] Moreover, TargetScanHuman 8.0 was utilized to predict the interaction/binding site between PARP-1 and miR-17-5p.

Statistical Analysis

All experiments were conducted at least three replicates and statistically analyzed by Student's t-test using GraphPad Prism 8 Software (San Diego, CA, USA). The results were expressed as mean ± SD. * P-value < .05, ** P-value < .01, *** P-value < .001, and **** P-value < .0001 were considered statistically significant.
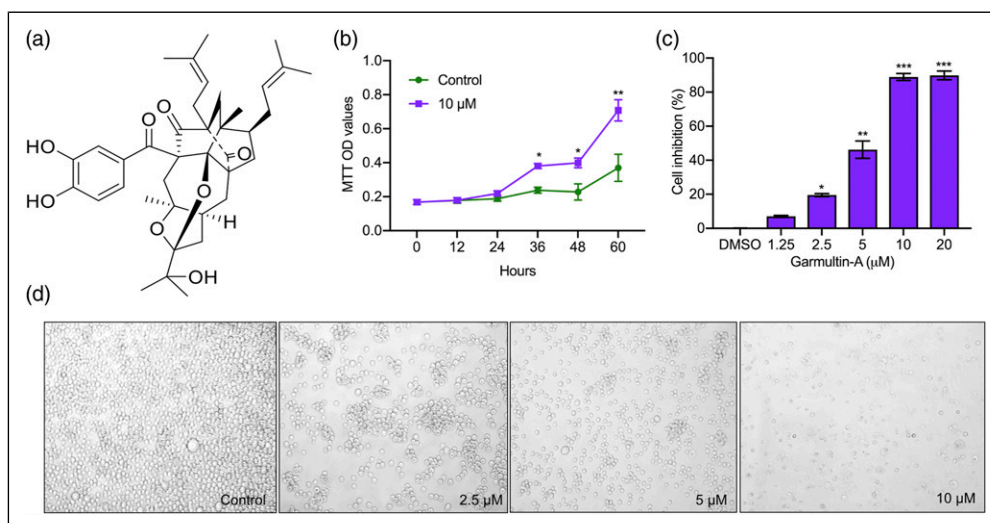
Figure 1. Effect of GA on the viability of CB3 cells. (A) Chemical structure of GA. (B) Cellular viability of CB3 treated with 10 μM GA for different time intervals. (C) The growth inhibition rate of CB3 cells treated with indicated concentrations for 48 h using MTT assay. (D) Effect of GA on the morphology of the CB3 cells (×20 magnification). Values are expressed as means ± SD of three independent experiments. * $P < .05$, ** $P < .01$, and *** $P < .001$ vs control.

Results

GA Administration Impaired CB3 Cell Viability

After 48 h of incubation with GA (Figure 1A), the cellular viability of CB3 cells was found to be reduced both in a time- and dose-dependent manner. The growth curve analysis revealed that the cell viability drastically deteriorated after 48 h of incubation (Figure 1B). The CB3 cells were administered with various concentrations of the compound for 48 h, to analyze the GA effect on cell viability. The cells were affected significantly from 2.5 μM treatment, with an IC_{50} value of 5.0 μM (Figure 1C). Moreover, the cellular loss dose-dependently found in trypan blue analysis (Additional file 1). The cellular morphology analysis revealed that GA was able to cause a dose-dependent cellular shrinkage and loss of the cells when compared with the DMSO control group (Figure 1D). Moreover, the cytotoxicity analysis of GA on normal liver cell line HL-7702 failed to show significant cellular toxicity at the selected doses of the drug, after 48 h of incubation (Additional file 2).

GA Induces Apoptosis in CB3 Cells and Causes Nuclear Loss

For studying the apoptosis-inducing effect of GA, CB3 cells with different doses of the compound (2.5, 5, and 10 μM) for 24 or 48 h were analyzed. The CB3 cells after GA treatment were analyzed by FITC Annexin V/PI staining using flow cytometry for its action on cellular apoptosis. The flow cytometry results showed that GA induced apoptosis in CB3 cells in a dose- and time-dependent manner. Even though there was a little effect on CB3 cells after 24 h treatment with 5 and 10 μM of GA, the apoptotic rate was observed to be highly significant after 48 h of incubation. At this juncture, the treatment of cells with 5 μM of GA significantly increased the apoptosis rate to $45.8 \pm 2.13\%$ from $22.2 \pm 1.32\%$ (at 24 h of incubation). Similarly, 10 μM treatment increased the apoptotic rate from $92.6 \pm 3.27\%$ to $98.7 \pm 4.25\%$. However, in DMSO control cells, apoptotic rates were $2.67 \pm .51\%$ and $4.5 \pm .32\%$, respectively, after 24 and 48 h of incubation (Figures 2A and 2B). To further confirm whether apoptosis caused nuclear loss, Hochest 33258 staining was performed. It revealed that the drug was able to create a dose- and time-dependent loss of the nucleus. It even showed that nuclear condensation was affected by the formation of apoptotic bodies and cellular apoptosis, after GA treatment (Figures 2C and 2D).

Effect of GA on Protein Expression of Onco- and Tumor Suppressor Proteins in CB3 Cells

For determining the molecular targets of apoptosis in CB3 cells, after GA treatment, the expression was analyzed for onco- and tumor suppressor proteins. The results demonstrated that GA treatment could significantly downregulate BCL2, cMYC, pERK, and PARP-1 protein levels. Similarly, it upregulated the BAX protein level expressions in a dose-dependent manner when compared with the DMSO control cells (Figure 2D).

Ligand–Protein Interaction Predictions Using Autodocking Analysis

The molecular interactive sites of the downregulated proteins were investigated by autodocking. The interacting amino
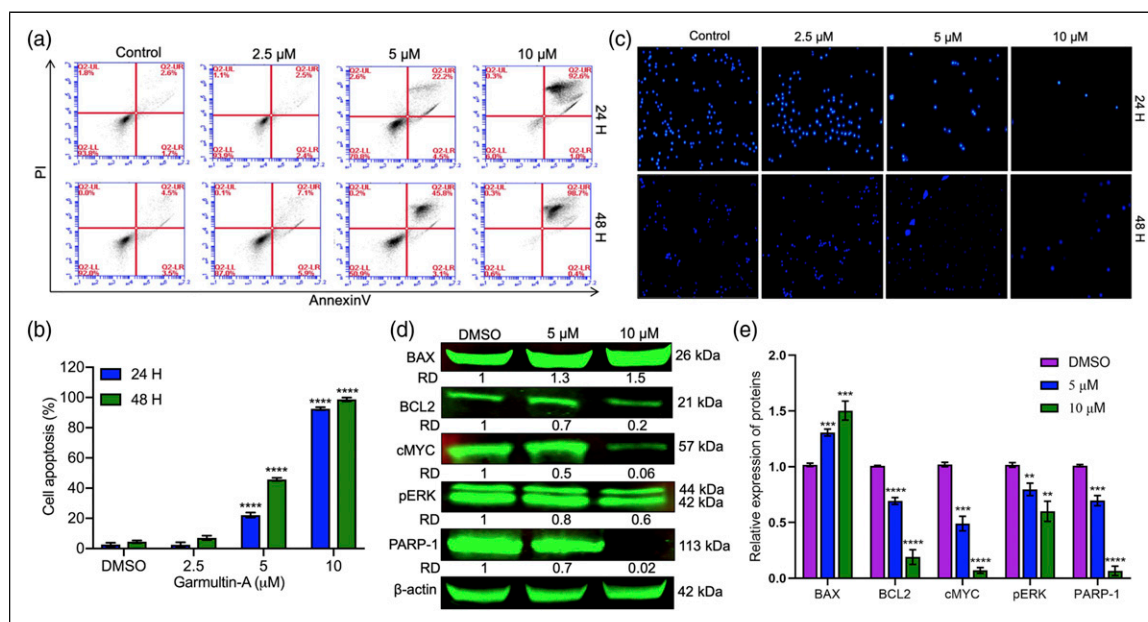
Figure 2. GA causes early and late apoptosis in CB3 cells. (A) CB3 cells were treated with indicated concentrations of GA for 24 and 48 h. After FITC Annexin V/PI double staining, the apoptosis ratios were analyzed by flow cytometry. (B) Quantification of apoptotic cell populations. Values are signified as means ± SD of triplicate independent experiments. **** *P* < .001 vs control. (C) Effect of GA on CB3 cell morphology and chromatin condensation evaluated by Hoechst staining magnification ×20). (D) Western blot analysis of indicated proteins in GA-treated cells at indicated concentrations (μM). (E) Densitometric analysis of protein expressions keeping β-actin as standard.

acids in the concerned proteins were depicted in 3D interaction images (Figures 3A, 3C, and 3E). The ligand was predicted to develop several favorable interactive sites with BCL2, cMYC, as well as pERK, namely, conventional hydrogen bonds, carbon-hydrogen bonds, van der Waals forces, attractive charged bonds, alkyl, and pi-Alkyl bonds (Figures 3B, 3D, and 3F). The study revealed that the binding energy values of GA with BCL2, cMYC, and pERK were predicted as −8.5, −11.1, and −8.3 Kcal/Mol (Figure 3G) with ligand efficacy of .06, .05, and .03, respectively. The interaction was much favorable with relatively better binding energy than the already known BCL2 (Additional file 3), cMYC (Additional file 4), and pERK (Additional file 5) inhibitors. The well-known inhibitors venetoclax, MLS006011554, and ravoxertinib showed only −7.4, −6.2, and −7.3 Kcal/mol of binding energies (Additional file 6) with corresponding ligand efficiencies as .02, .03, and .01, which is relatively less, compared to GA interactions. The most crucial finding was that none of the favorable interaction was observed between the PARP-1 and the ligand. It led us to think that the drug was unable to interact directly with PARP-1 but could indirectly downregulate its expression. It led us to work on miR-17-92 cluster genes, which are targets for alleviating PARP-1.

GA Induces miR-17-5p Overexpression

To determine whether miR-17-92 cluster genes are involved in anti-leukemia action, miR-17-5p levels were analyzed, viz,

qPCR analysis upon treatment with GA. MiR-17-5p expression significantly upregulated in CB3 cells treated with GA compared with the DMSO group (*P* < .001; Figure 4A) unless other genes were involved in the cluster. Interestingly, this suggested a possible targeting relationship between miR-17-5p and the PARP-1 protein.

Altered MiR-17-5p by GA Downregulates Expression of PARP-1

The study revealed that the 3′UTR of PARP-1 is the potential target of miR-17-5p (Figure 4B). Luciferase assays with NIH-3T3 cells transiently transfected with a reporter plasmid containing binding sites, along with vector miR-17-5p expression, were consistent with regulation of PARP-1 by miR-17-5p. Mutation of the binding sites for miR-17-5p, in PARP-1, restored luciferase activity (Figure 4C). The level of PARP-1 in the cells decreased after vector transfection with miR-17-5p (Figures 4D and 4E). Overexpression of miR-17-5p in CB3 cells significantly increased GA-induced apoptosis, compared with control (Figure 4F). Conversely, infection with antisense miR-17-5p vector decreased GA-induced apoptosis significantly (Figure 4G).

Discussion

The natural products have always been a choice of great interest for experimentation by the scientist to treat various ailments. In
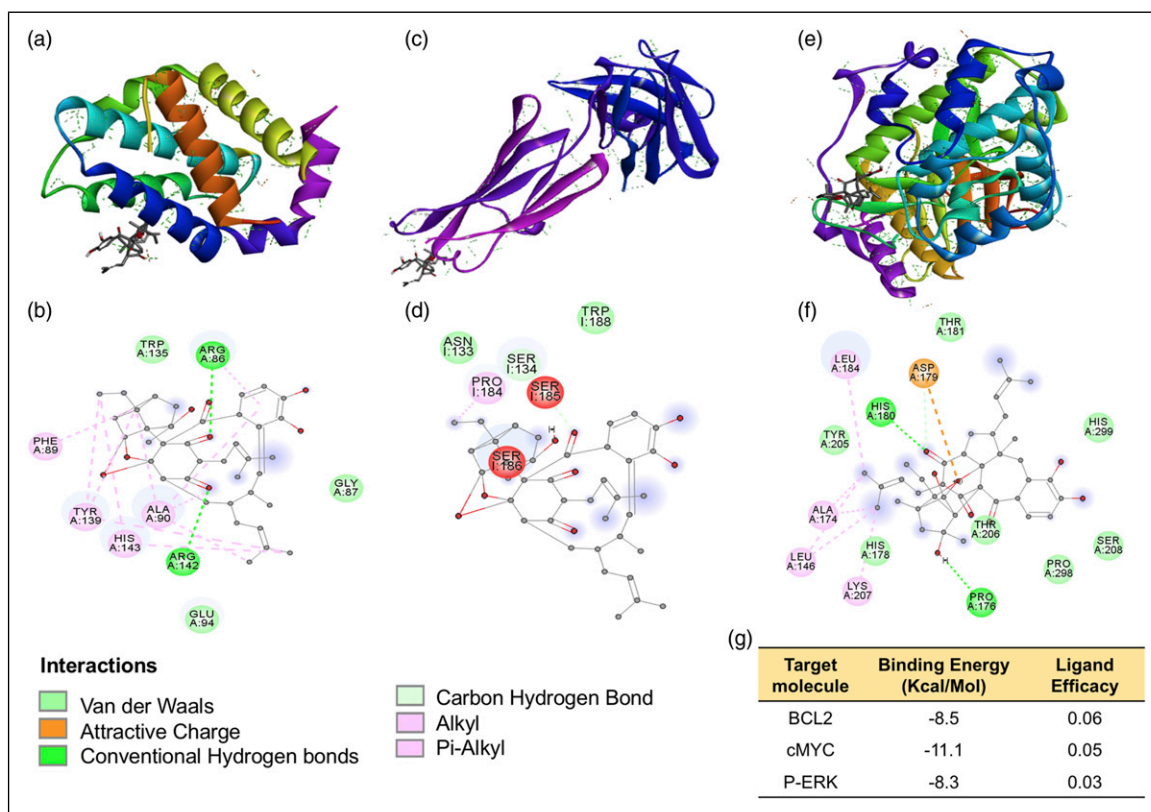
Figure 3. GA inhibits expression of BCL2, cMYC, and pERK. The 3-dimensional interactive images between GA and (A) BCL2, (C) cMYC, and (E) pERK. The 2-dimensional interactive plot between GA and (B) BCL2, (D) cMYC, and (F) pERK, showing prospective interactive forces and molecules of interactions of ligand to corresponding amino acids. (G) Binding energies and ligand efficacies of the indicated interacting molecules, analyzed by autodocking.

the same fashion, ruling out of the potential molecular targets of the bioactive compounds remains a challenging job. Thus, in this study, we have attempted to figure out the molecular target of GA in CB3 mouse erythroleukemia cells, which demonstrated prominent anticancer action.

The cell viability analysis proved that the compound could cause cell death in a dose- and time-dependent manner in CB3 cells. Further, the study revealed that cellular loss is mainly due to the apoptosis process after GA treatments. Our previous work has identified that GA could selectively kill various cancer cells via unknown mechanisms of action 6.

Possessing a piece of defective apoptotic machinery leads to uncontrolled proliferation. There are two types of death models for apoptosis: the extrinsic (mitochondrial independent) and the intrinsic pathway (mitochondrial independent). Alternation in BAX/BCL2 ratio accounts for the intrinsic type of apoptosis mechanism.[25] Likewise, in this study, we could see that the GA-treated cells had a variation in their BAX/BCL2 ratio compared to the control cells.

Moreover, cMYC promotes cell proliferation and impair cell apoptosis by activating or repressing the growth-promoting genes or growth-suppressing genes.[26] Inhibition of PARP-1 could modulate the cMYC-induced cell process.[27]

Moreover, that activation of PARP-1 is associated with ERK-mediated cell proliferation, apoptosis, and migration.[28] Inhibition of PARP-1 could impair BCL2 expressing tumor cells, which are resistant to apoptosis.[29] Likewise, our data proved that there was a downregulation of PARP-1, after GA administration, resulting in the reduction of cMYC, BCL2, and pERK, as well.

However, on the contrary, this study provides an insight into the interplay between miR-17-5p and PARP-1 in GA-induced apoptotic cell death. Most of the cancer cells can overcome apoptosis via the activation of PARP-1, which can repair both single-stranded and double-stranded DNA breaks.[27] The inhibition of PARP-1 results in a vast amount of DNA damage in cancer cells and apoptosis follows as the genetic mutations reach a lethal level.[28] The above studies are consistent with our finding that GA promotes apoptosis with a significant decrease of PARP-1 in CB3 cells. However, the autodock analysis failed to reveal a direct interaction between PARP-1 and GA, which made us think about the alternative target of the drug, causing downregulation of PARP-1 levels, which could be the miR-17-5p.

Specific overexpression of miR-17-5p blocks tumor cell proliferation and promotes apoptosis by directly targeting
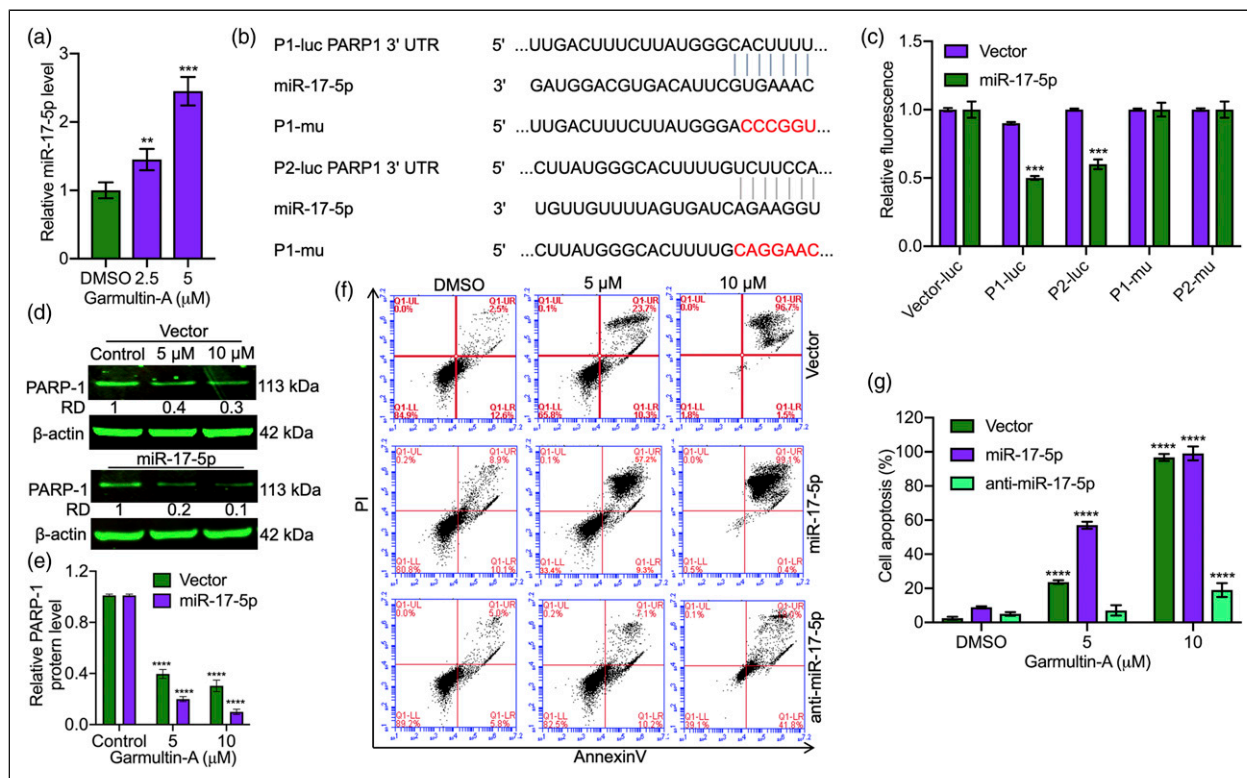
Figure 4. GA induces miR-17-5p overexpression coupled with alteration of expression of PARP-1 in CB3 cells. (A) The expression levels of miR-17-5p using q-PCR, after 48 h of GA (5 µM) incubation. (B) Schematic representation of the PARP-1 3′UTR sequence containing potential miR-17-5p binding sites (P1 and P2). Positions of mutations generated within P1 (P1-mu) and P2 (P2-mu) are marked in gray. (C) Luciferase assay of the reporter genes containing the P1 or P2 binding sites and their corresponding mutations (P1-mu or P2-mu) after transient transfection in NIH-3T3 cells stably expressing miR-17-5p. The expression is presented relative to that obtained with the transfection of the control vector alone. (D) CB3 cells infected with lentiviruses expressing a scrambled vector control and miR-17-5p, treated with indicated concentrations of GA or control DMSO. (E) Densitometric analysis of concerned protein expressions normalized with β-actin. (F) CB3 cells infected with lentiviruses expressing scramble vector, miR-17-5p, and antisense miR-17-5p analyzed for apoptosis by flow cytometry after 48 h, treated with indicated concentrations of GA or control DMSO. (G) Quantification of apoptosis ratios analyzed by flow cytometry. Values are signified as means ± SD of triplicate independent experiments. ** $P < .01$, *** $P < .001$, and **** $P < .0001$ vs control/vector.

oncogenes.[15] The miR-17-92 cluster encodes six miRNAs: miR-17, miR-19a, miR-18, miR-19b, miR-20, and miR-92. As oncogenes, these miRNAs promote cell proliferation, block apoptosis, and induce tumor angiogenesis.[30,31] However, the miR-17-5p, in exceptional cases, negatively regulates cell proliferation, inhibiting cell migration leading to invasion.[32] We have previously found that miR-17-5p can promote apoptosis by targeting BCL2 in leukemia cells.[32] The miR-17-5p can even inhibit cMYC-induced cell proliferation by functioning as a tumor suppressor in many cancer cells.[32] A recent study showed that the cMYC translation was down-regulated by miR-17-5p, in lymphoma cells.[33] Here, we also showed that overexpression of miR-17-5p could directly promote CB3 cell apoptosis and significantly enhance GA-induced apoptosis by reducing PARP-1 levels. It reported that knockdown of PARP-1 inhibited cancer cell proliferation, induced cancer cell apoptosis by reducing BCL2, and led to inactivation of the ERK1/2 signaling pathway.[34] The

inhibition of PARP-1 could suppress cMYC-mediated transactivation.[35] The PARP-1 inhibition increased the BAX promoter activation which could promote cell apoptosis. The overexpressed PARP-1 is observed in various types of breast, lung, hepatocellular, gastric, and leukemia cancers.[36] Also, it has been reported that the PARP-1 expression level can be a prognostic indicator and is related to a poor survival prognosis. PARP-1 inhibition was shown to be a useful aid to enhance cancer patients' survival rates.[36] Here, we suggest that GA-mediated overexpression of miR-17-5p promotes cell apoptosis by downregulating expression of PARP-1, BCL2, and cMYC and upregulating expression of BAX in CB3 cells. This mechanism adds to previous mechanisms of miR-17-5p action as a tumor suppressor in leukemic cells.[24] In our study, we could see that there was a significant elevation in the expression of miR-17-5p, after GA treatment. However, the luciferase assay showed that the knockdown of 3′UTR of the MiR-17-5p restored the fluorescence. Moreover, the
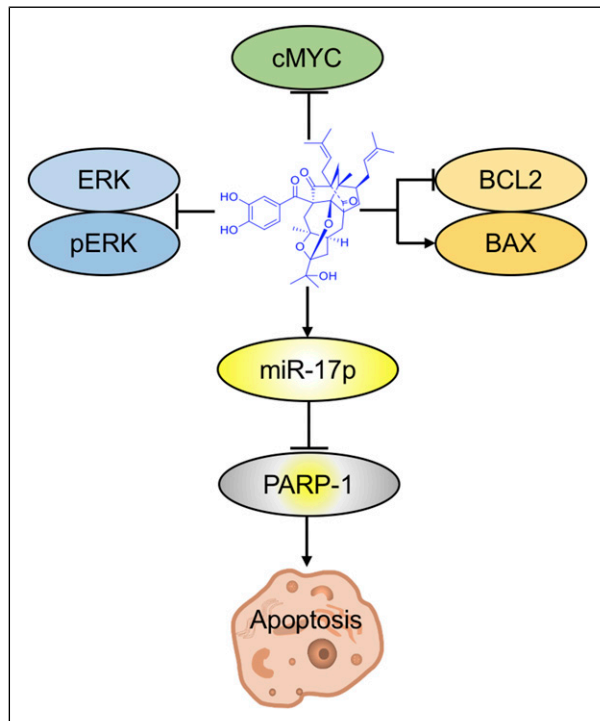
Figure 5. Schematic representation of the proposed mechanism of action of GA in CB3 cells.

anti-MiR-17-5p significantly restored the GA-triggered apoptosis. This could clearly rule out the role of miR-17-5p in GA-induced apoptosis.

Thus, the study reveals that the treatment with GA in CB3 cells could cause apoptosis and nuclear damage in a dose- and time-dependent manner. The drug, entering the cytoplasm, alters the BAX/BCL2 ratio (Figure 5). The drug could even inhibit the expression levels of cMYC and pERK molecules. On the other hand, the bioactive compound could enhance the expression of miR-17-5p, causing diminished expression levels of PARP-1. All these molecular machineries work together for apoptosis in the mouse erythroleukemia cells.

Conclusion

The present study revealed that miR-17-5p-mediated apoptotic signaling contributed to the GA-induced cellular apoptosis in CB3 erythroleukemia cells. The study suggested that miR-17-5p may be a promising target for natural compounds by attenuation of PARP-1, causing apoptosis. Thus, the study reveals that GA could be a viable drug of choice to treat erythroleukemia.

Declaration of Conflicting Interests

The author(s) declared no potential conflicts of interest with respect to the research, authorship, and/or publication of this article.

ORCID iD

Yanmei Li 🔟 https://orcid.org/0000-0003-3547-3492

Supplemental Material

Supplemental material for this article is available online.

References

1. Biersack B. Non-coding RNA/microRNA-modulatory dietary factors and natural products for improved cancer therapy and prevention: Alkaloids, organosulfur compounds, aliphatic carboxylic acids and water-soluble vitamins. *Noncoding RNA Res*. 2016;1(1):51-63.
2. Kedhari Sundaram M, Hussain A, Haque S, Raina R, Afroze N. Quercetin modifies 5'CpG promoter methylation and reactivates various tumor suppressor genes by modulating epigenetic marks in human cervical cancer cells. *J Cell Biochem*. 2019;120(10): 18357-18369. doi: 10.1002/jcb.29147. Epub 2019 Jun 6. PMID: 31172592.
3. Sala-Cirtog M, Marian C, Anghel A. New insights of medicinal plant therapeutic activity-The miRNA transfer. *Biomed Pharmacother*. 2015;74:228-232.
4. Palmer JD, Soule BP, Simone BA, Zaorsky NG, Jin L, Simone NL. MicroRNA expression altered by diet: Can food be medicinal? *Ageing Res Rev*. 2014;17:16-24.
5. Biersack B. Current state of phenolic and terpenoidal dietary factors and natural products as non-coding RNA/microRNA modulators for improved cancer therapy and prevention. *Noncoding RNA Res*. 2016;1(1):12-34.
6. Hong M, Wang N, Tan HY, Tsao SW, Feng Y. MicroRNAs and Chinese medicinal herbs: New possibilities in cancer therapy. *Cancers*. 2015;7(3):1643-1657.
7. Chi Y, Zhan XK, Yu H, et al. An open-labeled, randomized, multicenter phase IIa study of gambogic acid injection for advanced malignant tumors. *Chin Med J (Engl)*. 2013;126(9): 1642-1646.
8. Tian DS, Yi P, Xia L, et al. Biogenetically related polycyclic acylphloroglucinols from garcinia multiflora. *Org Lett*. 2016; 18(22):5904-5907.
9. Bartel DP. MicroRNAs: Genomics, biogenesis, mechanism, and function. *Cell*. 2004;116(2):281-297.

10. Friedman RC, Farh KK, Burge CB, Bartel DP. Most mammalian mRNAs are conserved targets of microRNAs. *Genome Res*. 2009;19(1):92-105.

11. Bartel DP. MicroRNAs: Target recognition and regulatory functions. *Cell*. 2009;136(2):215-233.

12. Mogilyansky E, Rigoutsos I. The miR-17/92 cluster: A comprehensive update on its genomics, genetics, functions and increasingly important and numerous roles in health and disease. *Cell Death Differ*. 2013;20(12):1603-1614.

13. Zhou L, Qi RQ, Liu M, et al. microRNA miR-17-92 cluster is highly expressed in epidermal Langerhans cells but not required for its development. *Genes Immun*. 2014;15(1):57-61.

14. Hayashita Y, Osada H, Tatematsu Y, et al. A polycistronic microRNA cluster, miR-17-92, is overexpressed in human lung cancers and enhances cell proliferation. *Cancer Res*. 2005;65(21):9628-9632.

15. Zhang L, Huang J, Yang N, et al. microRNAs exhibit high frequency genomic alterations in human cancer. *Proc Natl Acad Sci U S A*. 2006;103(24):9136-9141.

16. Zhang B, Pan X, Cobb GP, Anderson TA. microRNAs as oncogenes and tumor suppressors. *Dev Biol*. 2007;302(1):1-12.

17. Qiu Y, Yu Y, Qin XM, et al. CircTLK1 modulates sepsis-induced cardiomyocyte apoptosis via enhancing PARP1/HMGB1 axis-mediated mitochondrial DNA damage by sponging miR-17-5p. *J Cell Mol Med*. 2021;25(17):8244-8260.

18. Gajendran B, Varier KM, Liu W, et al. A C21-steroidal derivative suppresses T-cell lymphoma in mice by inhibiting SIRT3 via SAP18-SIN3. *Commun Biol*. 2020;3(1):732.

19. Mosmann T. Rapid colorimetric assay for cellular growth and survival: Application to proliferation and cytotoxicity assays. *J Immunol Methods*. 1983;65(1-2):55-63.

20. Varier KM, Sumathi T. Hinokitiol offers neuroprotection against 6-OHDA-induced toxicity in SH-SY5Y neuroblastoma cells by downregulating mRNA expression of MAO/α-synuclein/LRRK2/PARK7/PINK1/PTEN genes. *Neurotox Res*. 2019;35(4):945-954.

21. Lin X, Gajendran B, Varier KM, et al. Paris saponin VII induces apoptosis and cell cycle arrest in erythroleukemia cells by a mitochondrial membrane signaling pathway. *Anti Cancer Agents Med Chem*. 2021;21(4):498-507.

22. Gajendran B, Durai P, Madhu Varier K, Chinnasamy A. A novel phytosterol isolated from Datura inoxia, RinoxiaB is a potential cure colon cancer agent by targeting BAX/Bcl2 pathway. *Bioorg Med Chem*. 2020;28(2):115242.

23. Krishnapriya MV, Sumathi T, Arulvasu C, Gopalsamy B, Renjith P. Comparative analysis of potentiality of esculin and hinokitol (β-thujaplicin) as anti-parkinsonism drugs: A pilot *in silico* study. *Int J Pharm Pharm Sci*. 2016;9(1):108-115.

24. Li Y, Vecchiarelli-Federico LM, Li YJ, et al. The miR-17-92 cluster expands multipotent hematopoietic progenitors whereas imbalanced expression of its individual oncogenic miRNAs promotes leukemia in mice. *Blood*. 2012;119(19):4486-4498.

25. Sun H, Hou H, Lu P, et al. Isocorydine inhibits cell proliferation in hepatocellular carcinoma cell lines by inducing G2/m cell cycle arrest and apoptosis. *PLoS One*. 2012;7(5):e36808.

26. Pyndiah S, Tanida S, Ahmed KM, Cassimere EK, Choe C, Sakamuro D. c-MYC suppresses BIN1 to release poly(ADP-ribose) polymerase 1: A mechanism by which cancer cells acquire cisplatin resistance. *Sci Signal*. 2011;4(166):ra19.

27. Langelier MF, Pascal JM. PARP-1 mechanism for coupling DNA damage detection to poly(ADP-ribose) synthesis. *Curr Opin Struct Biol*. 2013;23(1):134-143.

28. Cohen-Armon M. PARP-1 activation in the ERK signaling pathway. *Trends Pharmacol Sci*. 2007;28(11):556-560.

29. Dutta C, Day T, Kopp N, et al. BCL2 suppresses PARP1 function and nonapoptotic cell death. *Cancer Res*. 2012;72(16):4193-4203.

30. Grillari J, Hackl M, Grillari-Voglauer R. miR-17-92 cluster: Ups and downs in cancer and aging. *Biogerontology*. 2010;11(4):501-506.

31. Olive V, Jiang I, He L. mir-17-92, a cluster of miRNAs in the midst of the cancer network. *Int J Biochem Cell Biol*. 2010;42(8):1348-1354.

32. Hossain A, Kuo MT, Saunders GF. Mir-17-5p regulates breast cancer cell proliferation by inhibiting translation of AIB1 mRNA. *Mol Cell Biol*. 2006;26(21):8191-8201.

33. Mihailovich M, Bremang M, Spadotto V, et al. miR-17-92 fine-tunes MYC expression and function to ensure optimal B cell lymphoma growth. *Nat Commun*. 2015;6:8725.

34. Ethier C, Labelle Y, Poirier GG. PARP-1-induced cell death through inhibition of the MEK/ERK pathway in MNNG-treated HeLa cells. *Apoptosis*. 2007;12(11):2037-2049.

35. Chiou SH, Jiang BH, Yu YL, et al. Poly(ADP-ribose) polymerase 1 regulates nuclear reprogramming and promotes iPSC generation without c-Myc. *J Exp Med*. 2013;210(1):85-98.

36. Mazzotta A, Partipilo G, De Summa S, Giotta F, Simone G, Mangia A. Nuclear PARP1 expression and its prognostic significance in breast cancer patients. *Tumour bio: The J In Soc Onco Dev Bio Med* 2016;37(5):6143-6153.